

**Momentum dependence of the  $\phi$ -meson nuclear transparency**

M. Hartmann,<sup>1,\*</sup> Yu. T. Kiselev,<sup>2,†</sup> A. Polyanskiy,<sup>1,2</sup> E. Ya. Paryev,<sup>3</sup> M. Büscher,<sup>1</sup> D. Chiladze,<sup>1,4</sup> S. Dymov,<sup>5,6</sup> A. Dzyuba,<sup>7</sup> R. Gebel,<sup>1</sup> V. Hejny,<sup>1</sup> B. Kämpfer,<sup>8</sup> I. Keshelashvili,<sup>9</sup> V. Koptev,<sup>7,‡</sup> B. Lorentz,<sup>1</sup> Y. Maeda,<sup>10</sup> V. K. Magas,<sup>11</sup> S. Merzliakov,<sup>1,6</sup> S. Mikirtychiants,<sup>1,7</sup> M. Nikipelov,<sup>1</sup> H. Ohm,<sup>1</sup> L. Roca,<sup>12</sup> H. Schade,<sup>8,13</sup> V. Serdyuk,<sup>1,6</sup> A. Sibirtsev,<sup>5</sup> V. Y. Sinitsyna,<sup>14</sup> H. J. Stein,<sup>1</sup> H. Ströher,<sup>1</sup> S. Trusov,<sup>8,15</sup> Yu. Valdau,<sup>1,16</sup> C. Wilkin,<sup>17</sup> P. Wüstner,<sup>18</sup> and Q. J. Ye<sup>19</sup>

<sup>1</sup>*Institut für Kernphysik and Jülich Centre for Hadron Physics, Forschungszentrum Jülich, D-52425 Jülich, Germany*

<sup>2</sup>*Institute for Theoretical and Experimental Physics, RU-117218 Moscow, Russia*

<sup>3</sup>*Institute for Nuclear Research, Russian Academy of Sciences, RU-117312 Moscow, Russia*

<sup>4</sup>*High Energy Physics Institute, Tbilisi State University, GE-0186 Tbilisi, Georgia*

<sup>5</sup>*Physikalisches Institut, Universität Erlangen-Nürnberg, D-91058 Erlangen, Germany*

<sup>6</sup>*Laboratory of Nuclear Problems, Joint Institute for Nuclear Research, RU-141980 Dubna, Russia*

<sup>7</sup>*High Energy Physics Department, Petersburg Nuclear Physics Institute, RU-188350 Gatchina, Russia*

<sup>8</sup>*Institut für Kern- und Hadronenphysik, Helmholtz-Zentrum Dresden-Rossendorf, D-01314 Dresden, Germany*

<sup>9</sup>*Department of Physics, University of Basel, CH-4056 Basel, Switzerland*

<sup>10</sup>*Research Center for Nuclear Physics, Osaka University, Ibaraki, Osaka 567-0047, Japan*

<sup>11</sup>*Departament d'Estructura i Constituents de la Matèria and Institut de Ciències del Cosmos, Universitat de Barcelona, E-08028 Barcelona, Spain*

<sup>12</sup>*Departamento de Física, Universidad de Murcia, E-30071 Murcia, Spain*

<sup>13</sup>*Institut für Theoretische Physik, TU Dresden, D-01062 Dresden, Germany*

<sup>14</sup>*P. N. Lebedev Physical Institute, RU-119991 Moscow, Russia*

<sup>15</sup>*Skobel'syn Institute of Nuclear Physics, Lomonosov Moscow State University, RU-119991 Moscow, Russia*

<sup>16</sup>*Helmholtz-Institut für Strahlen- und Kernphysik, Universität Bonn, D-53115 Bonn, Germany*

<sup>17</sup>*Physics and Astronomy Department, UCL, London WC1E 6BT, United Kingdom*

<sup>18</sup>*Zentralinstitut für Elektronik, Forschungszentrum Jülich, D-52425 Jülich, Germany*

<sup>19</sup>*Department of Physics and Triangle Universities Nuclear Laboratory, Duke University, Durham, North Carolina 27708, USA*

(Received 17 January 2012; published 19 March 2012)

The production of  $\phi$  mesons in proton collisions with C, Cu, Ag, and Au targets has been studied via the  $\phi \rightarrow K^+ K^-$  decay at an incident beam energy of 2.83 GeV using the ANKE detector system at COSY. For the first time, the momentum dependence of the nuclear transparency ratio, the in-medium  $\phi$  width, and the differential cross section for  $\phi$ -meson production at forward angles have been determined for these targets over the momentum range of 0.6–1.6 GeV/c. There are indications of a significant momentum dependence in the value of the extracted  $\phi$  width, which corresponds to an effective  $\phi N$  absorption cross section in the range of 14–21 mb.

DOI: [10.1103/PhysRevC.85.035206](https://doi.org/10.1103/PhysRevC.85.035206)

PACS number(s): 13.25.-k, 13.75.-n, 14.40.Be

**I. INTRODUCTION**

The study of the effective masses and widths of light vector mesons  $\rho$ ,  $\omega$ , and  $\phi$  in a nuclear medium, through their production and decay in the collisions of photon, hadron, and heavy-ion beams with nuclear targets, has received considerable attention in recent years (see, for example, Refs. [1–3]). This interest in the in-medium properties was triggered by the hypothesis of universal scaling of Brown and Rho [4], as well as by the QCD-sum-rule-based prediction of Hatsuda and Lee [5] that the masses of these mesons should be lower in nuclear matter due to the partial restoration of chiral symmetry in hot and dense nuclear matter. This is a fundamental symmetry of QCD in the limit of vanishing quark masses, and its restoration would be characterized by

a reduction of the scalar quark condensate in the medium compared to its magnitude in vacuum.

The natural width of the  $\phi(1020)$  meson is only 4.3 MeV/c<sup>2</sup>, which is narrow compared to other nearby resonances. It is therefore the optimal probe for the investigation of medium modifications because small effects should be experimentally observable. However, this meson is of interest for other reasons. Since the  $\phi$  is an almost pure  $s\bar{s}$  state, the Okubo-Zweig-Iizuka (OZI) rule [6] suppresses quark exchange in its interaction with ordinary (nonstrange) baryonic matter. Gluon exchange, which plays a substantial role in high-energy interactions between hadrons, is therefore expected to dominate  $\phi N$  scattering at all energies [7]. The  $\phi$  might therefore be considered a *clean* system for the study of gluonic exchange which, at low energies, should manifest itself as an attractive QCD van der Waals force, which could even lead to the formation of  $\phi N$  bound states [8]. In addition, owing to the small energy release in the dominant  $K\bar{K}$  decay channel, any changes in the  $\phi$  properties are very sensitive to

\*m.hartmann@fz-juelich.de

†yurikis@itep.ru

‡Deceased

possible in-medium modifications of kaons and antikaons, a subject which is also of great current interest.

The main modification of the  $\phi$  properties in nuclear matter is expected to be a broadening of its spectral function, while its mass should be hardly shifted [3,5,9–12]. Dileptons from  $\phi \rightarrow e^+e^-/\mu^+\mu^-$  decays experience no strong final-state interactions in a nucleus. Any broadening of the  $\phi$  line shape in the nuclear matter should be directly testable by examining dilepton mass spectra produced by elementary or heavy-ion beams, provided that the necessary cuts are applied at low  $\phi$  momenta [13,14]. However, the measurement of such spectra is difficult due to the low branching ratios for leptonic decays. Furthermore, their sensitivity to in-medium modifications will be reduced by the profile of the nucleus spanning all densities from zero to normal nuclear matter density  $\rho_0 = 0.16 \text{ fm}^{-3}$ , which smears out any density-dependent signal [3]. The KEK-PS-E325 Collaboration measured  $e^+e^-$  invariant mass distributions in the  $\phi$  region in proton-induced reactions on carbon and copper at 12 GeV and reported a mass shift of 3.4% and a width increase by a factor of 3.6 at density  $\rho_0$  for  $\phi$  momenta around 1 GeV/c [13].

An alternative way to determine the in-medium broadening of the  $\phi$  meson has been proposed in Ref. [12] and adopted in Refs. [15,16]. Here, the variation of the  $\phi$  production cross section (or nuclear transparency ratio) with atomic number  $A$  has been studied both experimentally and theoretically. The big advantage of this method is that one can exploit the dominant  $K^+K^-$  branching ratio ( $\approx 50\%$ ). The  $A$  variation depends on the attenuation of the  $\phi$  flux in the nucleus which, in turn, is governed by the imaginary part of the  $\phi$  in-medium self-energy or width. In the low-density approximation [17], this width can be related to an effective  $\phi N$  absorption cross section  $\sigma_{\phi N}$ , though this is less obvious at higher densities where two-nucleon effects might be significant.

A large in-medium  $\phi N$  absorption cross section of about 35 mb was inferred in a Glauber-type analysis by the LEPS Collaboration from measurements of  $K^+K^-$  pairs photoproduced on Li, C, Al, and Cu targets at SPring-8 for average  $\phi$  momenta  $\approx 1.8 \text{ GeV}/c$  [15]. Similar considerations were given in Ref. [18]. This large  $\phi N$  cross section was confirmed in BUU transport model calculations [19]. In the low-density approximation, this implies an in-medium  $\phi$  width of about  $110 \text{ MeV}/c^2$  in its rest frame at density  $\rho_0$  for the conditions of the KEK measurements [13]. This is clearly incompatible with the width reported in the KEK experiment. This value of  $\sigma_{\phi N}$  is also significantly larger than the  $\approx 10 \text{ mb}$  obtained from both photoproduction data on hydrogen, using the vector-meson dominance model in the photon energy range  $E_\gamma < 10 \text{ GeV}$  [18,20], and the additive quark model [21].

Values of the in-medium  $\sigma_{\phi N}$  were also determined by the CLAS Collaboration from transparency ratio measurements at JLab [16]. In this experiment, the  $\phi$  mesons were photoproduced on  $^2\text{H}$ , C, Ti, Fe, and Pb targets and detected via their  $e^+e^-$  decay mode. From an analysis of the transparency ratios normalized to carbon within a Glauber model, values of  $\sigma_{\phi N}$  in the range of 16–70 mb were extracted for an average  $\phi$  momentum of  $\approx 2 \text{ GeV}/c$ . These are to be compared to the free value of  $\approx 10 \text{ mb}$ .

The SPring-8 [15] and JLab [16] results are consistent with the JLab measurements of coherent [7] and incoherent [22]  $\phi$  photoproduction from deuterium. The coherent data suggest that  $\sigma_{\phi N} \approx 30 \text{ mb}$  together with a larger slope for elastic  $\phi N$  scattering compared to  $\gamma N \rightarrow \phi N$  [7]. A combined analysis of coherent and incoherent  $\phi$ -meson photoproduction from deuterium favors  $\sigma_{\phi N} > 20 \text{ mb}$  [22].

Whereas medium modifications of  $\sigma_{\phi N}$  might offer a plausible explanation of the SPring-8 [15] and JLab [16] data, they can hardly account for the large value found in deuterium. Nuclear density effects are here minimal and other mechanisms, beyond medium modifications, could be more important [22]. In this context it should be noted that the LEPS Collaboration recently studied incoherent  $\phi$  photoproduction from deuterium at forward angles for  $E_\gamma = 1.5\text{--}2.4 \text{ GeV}$  [23]. The nuclear transparency ratio, extracted as a function of  $E_\gamma$ , shows a significant 25%–30% reduction, which is consistent with that previously deduced by the same collaboration from the  $A$  dependence of this ratio for heavier nuclear targets [15]. On the other hand, very recent data on incoherent  $\phi$  photoproduction on deuterium, taken by the CLAS Collaboration in a similar photon energy range but over a region of larger momentum transfers [24], are inconsistent with the LEPS results [23].

The divergent conclusions drawn from the various experiments emphasize the need to improve our understanding of the  $\phi N$  interaction in nuclei. With the aim of furthering these studies, we have measured the inclusive production of  $\phi$  mesons at forward angles in the collisions 2.83 GeV protons with C, Cu, Ag, and Au targets. The meson was detected via the  $\phi \rightarrow K^+K^-$  decay using the ANKE-COSY magnetic spectrometer [25]. Values of the nuclear transparency ratio normalized to carbon,  $R = (12/A)(\sigma^A/\sigma^C)$ , were deduced, averaged over the  $\phi$  momentum range 0.6–1.6 GeV/c. Here  $\sigma^A$  and  $\sigma^C$  are inclusive cross sections for  $\phi$  production in  $pA$  ( $A = \text{Cu, Ag, and Au}$ ) and  $pC$  collisions in the angular cone  $\theta_\phi < 8^\circ$ . The comparison of the ratio with model calculations [26–28] yielded an in-medium  $\phi$  width of 33–50 MeV/c<sup>2</sup> in the nuclear rest frame for an average  $\phi$  momentum of 1.1 GeV/c for normal nuclear density  $\rho_0$ .

Because of the large number of reconstructed  $\phi$  mesons for each target (7000–10000), the data could be put in bins in order to obtain differential distributions. This allows us to carry out more detailed investigations, in particular of the momentum dependence of the parameters. In this paper we report on the results of further analysis of the data collected in our experiment [25,29].

## II. EXPERIMENT AND RESULTS

A series of thin and narrow C, Cu, Ag, and Au targets was inserted in a beam of 2.83 GeV protons, circulating in the COSY Cooler Synchrotron and storage ring of the Forschungszentrum Jülich, in front of the main spectrometer magnet D2 of the ANKE system (see Refs. [30,31]). The ANKE spectrometer has detection systems placed to the right and left of the beam to register positively and negatively charged ejectiles, which, in the case of  $\phi$ -meson production,

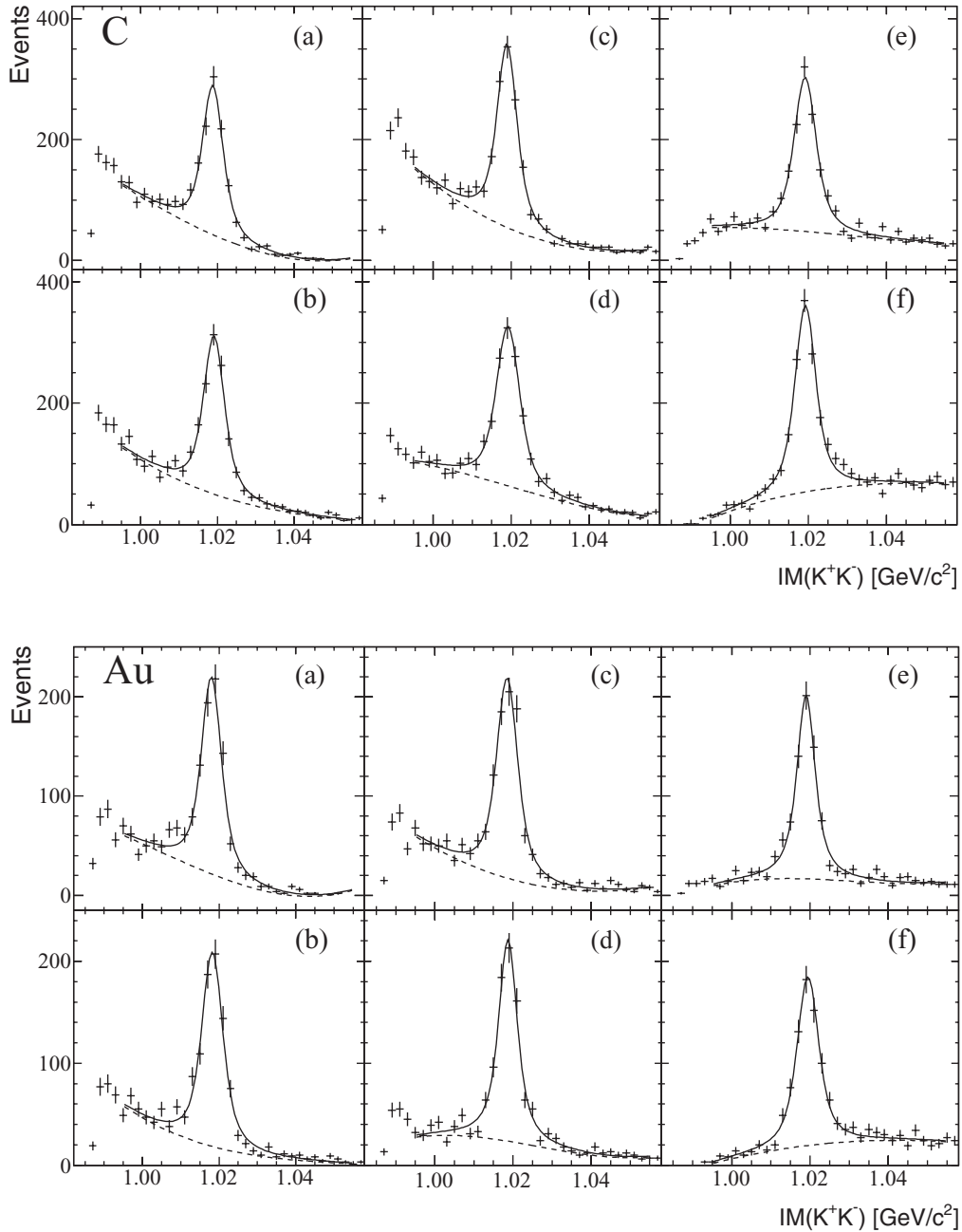


FIG. 1. Invariant mass distributions of  $K^+K^-$  pairs produced in  $pC$  and  $pAu$  collisions in the  $\phi$  momentum bins: (a) 0.600–0.825, (b) 0.825–0.950, (c) 0.950–1.075, (d) 1.075–1.200, (e) 1.200–1.325, and (f) 1.325–1.600 GeV/c. Fits to the uncorrected experimental data in terms of an expected  $\phi$  shape and a physical background are shown by the solid lines. The dashed lines are third-order polynomial parametrizations of the backgrounds in the region of the  $\phi$  peak.

are the  $K^+$  and  $K^-$ . Although only used here for efficiency studies, forward-going charged particles could also be measured in coincidence. The positively charged kaon was first selected using a dedicated detection system that can identify a  $K^+$  against a pion and/or proton background that is  $10^5$  times more intense [29,31,32]. The coincident  $K^-$  was subsequently identified from the time-of-flight difference between the stop counters in the negative and positive detector systems.

The accessible range of the  $\phi$ -meson momenta,  $0.6 < p_\phi < 1.6$  GeV/c, was divided into six intervals with about 1000

mesons per bin. The  $K^+K^-$  invariant mass spectra measured in the  $pA \rightarrow K^+K^-X$  reaction look similar for all four targets, and only the results for carbon and gold are presented in Fig. 1. In every case there is a clear  $\phi$  signal sitting on a background of mainly nonresonant kaon pair production together with a relatively small number of misidentified events. To study the momentum dependence of the transparency ratio  $R$ , the numbers of  $\phi$  events falling within each momentum bin were evaluated for the four targets. With this in mind, the mass spectra were fitted by the incoherent sum of a Breit-Wigner

TABLE I. The measured transparency ratio  $R$  in the acceptance window of the ANKE spectrometer for six momentum bins. The first errors are statistical and the second systematic, which are mainly associated with the fit quality. In addition there are overall systematic uncertainties in the ratios of about 5%–6%, coming principally from the relative normalizations.

$p_\phi$ (GeV/ $c$ )	$R(\text{Cu}/\text{C})$	$R(\text{Ag}/\text{C})$	$R(\text{Au}/\text{C})$
0.600–0.825	$0.49 \pm 0.03 \pm 0.03$	$0.48 \pm 0.03 \pm 0.03$	$0.34 \pm 0.02 \pm 0.02$
0.825–0.950	$0.48 \pm 0.03 \pm 0.04$	$0.39 \pm 0.03 \pm 0.03$	$0.32 \pm 0.02 \pm 0.02$
0.950–1.075	$0.48 \pm 0.03 \pm 0.03$	$0.39 \pm 0.03 \pm 0.03$	$0.31 \pm 0.02 \pm 0.02$
1.075–1.200	$0.49 \pm 0.03 \pm 0.04$	$0.40 \pm 0.03 \pm 0.03$	$0.30 \pm 0.02 \pm 0.02$
1.200–1.325	$0.42 \pm 0.03 \pm 0.03$	$0.35 \pm 0.02 \pm 0.02$	$0.27 \pm 0.02 \pm 0.01$
1.325–1.600	$0.41 \pm 0.02 \pm 0.02$	$0.31 \pm 0.02 \pm 0.02$	$0.24 \pm 0.01 \pm 0.01$

function with the natural  $\phi$  width, convoluted with a Gaussian resolution function with  $\sigma \approx 1$  MeV/ $c^2$ , and a polynomial background function.

Since the efficiency corrections in the ANKE spectrometer are essentially target-independent, after taking the luminosity into account, to a good approximation the ratio of the number of reconstructed  $\phi$  in any bin for a nucleus  $A$  to that for carbon corresponds to ratio of the cross sections for  $\phi$  production on these targets in the given momentum bin [25]. The resulting transparency ratios are given in Table I and shown in Fig. 2. For all the combinations, Cu/C, Ag/C, and Au/C,  $R$  falls when the  $\phi$  momentum increases.

Each momentum bin contains roughly equal numbers of events, and the associated statistical uncertainty in  $R$  is about 6%–7%. The main systematic effects arise from the evaluation of the number of  $\phi$  falling within a certain momentum bin and the overall uncertainty in the relative normalization. The first was estimated by varying the fit parameters, the binning of the histograms, the range of fitting, and the order of the polynomial background. These results are reported in Table I. The relative normalization uncertainty, which is described in detail in Refs. [25,29], is about 4%–6%, depending on the target nucleus.

In order to test further the model calculations, the double differential cross sections for  $\phi$ -meson production have been

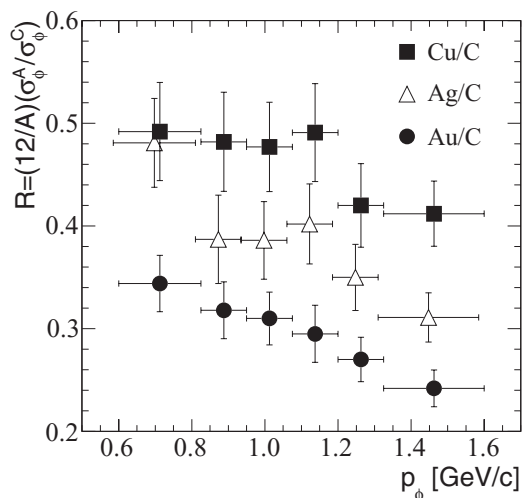


FIG. 2. Momentum dependence of the transparency ratio  $R$ , normalized to carbon, for Cu, Ag, and Au targets.

evaluated within the ANKE acceptance window for each momentum bin  $\Delta p$  and each nucleus  $A$  as

$$\frac{d^2\sigma_\phi^A}{dp d\Omega} = \frac{1}{(\Delta p \Delta \Omega)} \frac{N_\phi^A}{\langle \epsilon_\phi \rangle L_{\text{int}}^A}, \quad (1)$$

where  $N_\phi^A$  is the number of  $\phi$  detected in a solid angle  $\Delta \Omega$  and  $L_{\text{int}}^A$  is the integrated luminosity for target  $A$ . In order to estimate the average efficiency for  $\phi$  identification  $\langle \epsilon_\phi \rangle$ , the detection efficiency was first evaluated for each nucleus and each momentum bin. For this the ratio of the number of  $\phi$  detected to that determined from the fitting the  $K^+K^-$  efficiency-corrected invariant-mass distributions was calculated on an event-by-event basis. These efficiencies were then averaged over the target nuclei for each momentum bin. The root-mean-square deviations of the individual efficiencies from  $\langle \epsilon_\phi \rangle$  were about 5%, which is consistent with the statistical uncertainties.

The efficiency was estimated for each event using

$$\epsilon_\phi = \epsilon_{\text{tel}} \times \epsilon_{\text{tr}} \times \epsilon_{\text{acc}} \times \epsilon_{\text{BR}}. \quad (2)$$

The track reconstruction efficiency of  $K^+K^-$  pairs  $\epsilon_{\text{tr}}$  is determined from the experimental data. The correction for kaon decay in flight and acceptance ( $\epsilon_{\text{acc}}$ ) is determined as a function of the laboratory momentum and the laboratory polar angle of the  $\phi$  meson, using simulations and assuming an isotropic  $\phi$  decay in its rest frame. The range-telescope efficiency  $\epsilon_{\text{tel}}$  is extracted from calibration data on  $K^+p$  coincidences. Finally,  $\epsilon_{\text{BR}}$  represents the branching ratio of the  $\phi \rightarrow K^+K^-$  decay mode.

The integrated luminosity  $L_{\text{int}}^A$  is calculated using the measured flux of  $\pi^+$  mesons with momenta  $\approx 500$  MeV/ $c$  produced at small laboratory angles. Values of the  $\pi^+$  production cross sections used at 2.83 GeV are  $59.8 \pm 7.2$  for carbon,  $113 \pm 15$  for copper,  $138 \pm 19$  for silver, and  $174 \pm 24$  mb/(sr GeV/ $c$ ) for gold (the details are given in Ref. [33]).

The measured double differential cross section for  $\phi$  production for the four targets is given in Table II. The statistical uncertainties are about 5% for each momentum bin and nucleus. The overall systematic uncertainties are typically 20%, rising to 23% for the first and last momentum bins. The main sources of the systematic effects are related to the background subtraction in the  $K^+K^-$  invariant mass spectra (5%–10%), the simulation of acceptance corrections  $\epsilon_{\text{acc}}$  (5%–10%), the determination of the range-telescope efficiency

TABLE II. The measured double differential cross section  $d^2\sigma_\phi^A/(dp d\Omega)$  [ $\mu\text{b}/(\text{sr GeV}/c)$ ] for  $\phi$  production at small angles ( $\theta_\phi \leq 8^\circ$ ) for different momentum bins and nuclei. The first errors are statistical and the second systematic, which are associated with the fit quality and include the uncertainty in the average detection efficiency ( $\varepsilon_\phi$ ). In addition there are overall systematic uncertainties of about 20%–23%. For details, see the text.

$p_\phi$ (GeV/ $c$ )	C	Cu	Ag	Au
0.600–0.825	$9.9 \pm 0.4 \pm 0.9$	$26.2 \pm 1.3 \pm 2.7$	$43.3 \pm 2.0 \pm 4.3$	$58.0 \pm 2.4 \pm 5.2$
0.825–0.950	$13.3 \pm 0.6 \pm 0.8$	$34.4 \pm 1.7 \pm 2.4$	$46.6 \pm 2.3 \pm 4.0$	$72.0 \pm 3.0 \pm 4.0$
0.950–1.075	$14.5 \pm 0.6 \pm 1.0$	$37.3 \pm 1.8 \pm 2.6$	$51.0 \pm 2.3 \pm 4.0$	$76.8 \pm 3.0 \pm 4.9$
1.075–1.200	$15.3 \pm 0.7 \pm 1.5$	$40.3 \pm 1.8 \pm 3.2$	$55.8 \pm 2.7 \pm 4.4$	$76.7 \pm 3.1 \pm 6.0$
1.200–1.325	$18.1 \pm 0.8 \pm 1.0$	$40.9 \pm 2.1 \pm 2.6$	$57.8 \pm 2.8 \pm 3.4$	$83.5 \pm 3.8 \pm 3.4$
1.325–1.600	$18.7 \pm 0.7 \pm 0.9$	$41.4 \pm 1.9 \pm 1.8$	$53.1 \pm 2.4 \pm 2.2$	$77.2 \pm 3.4 \pm 2.9$

$\varepsilon_{\text{tel}}$  (10%), and the estimation of the integrated luminosity  $L_{\text{int}}^A$  (12%–14%).

### III. DISCUSSION

To interpret the data presented here, a reaction model is essential and, in the subsequent discussion, we consider three approaches.

*Model 1:* The eikonal approximation of the Valencia group [26] uses the predicted  $\phi$  self-energy in nuclear medium [11, 12] both for the one-step ( $pN \rightarrow pN\phi$ ) and two-step  $\phi$  production processes, with nucleon and  $\Delta$  intermediate states.

*Model 2:* Paryev [27] developed the spectral function approach for  $\phi$  production in both the primary proton-nucleon and secondary pion-nucleon channels.

*Model 3:* The BUU transport calculation of the Rossendorf group [28] accounts for a variety baryon-baryon and meson-baryon  $\phi$  production processes. In contrast to models 1 and 2, where  $\phi$  absorption is governed by its width  $\Gamma_\phi$ , model 3 describes it in terms of an effective in-medium  $\phi N$  absorption cross section  $\sigma_{\phi N}$  that can be related to the  $\phi$  width  $\Gamma_\phi$  within the low-density approximation.

One of the major differences between the three models is in the treatment of the secondary  $\phi$  production processes. In addition, in contrast to model 2, in model 3 a  $\phi$  mass shift of  $-22 \text{ MeV}/c^2$  at density  $\rho_0$  is considered. This results in a modest increase of the  $\phi$  production cross section in the range of 0.6–1.6 GeV/ $c$ .

The results of the calculations of the transparency ratio as functions of the  $\phi$  momentum are presented separately in the three columns of Fig. 3 for the different models. Curve 1 of model 1 results from using the predictions [12] for the imaginary part of the  $\phi$  self-energy in nuclear matter. The other curves, corresponding to calculations with this self-energy multiplied by factors of 0.5, 2, and 4, demonstrate the sensitivity of  $R$  to the value of the  $\phi$  width. Calculations within model 2 shown in the central panel were performed with different values of a momentum-independent width  $\Gamma_\phi$  of the  $\phi$  meson in its rest frame at density  $\rho_0$ . These values are

noted (in  $\text{MeV}/c^2$ ) next to the curves. Calculations in model 3 presented in the right panel were produced using the absorption cross section  $\sigma_{\phi N}$  (in mb) indicated. For comparison, the values of the experimental transparency ratios are also shown, but without error bars.

It is seen from Fig. 3 that, for an almost momentum-independent  $\phi$  self-energy, model 1 predicts a steady rise of the transparency ratios with laboratory  $\phi$  momentum, which is inconsistent with the steady fall in the data. Any momentum dependence in the results of model 2 is much more moderate but it is clear that in neither case can the variation of the Cu/C, Ag/C, and Au/C transparency ratios be described with a single value of the  $\phi$  width. The results from model 3 are more promising in this respect, since the steady fall in the data can be reproduced with a constant  $\phi N$  absorption cross section of about 15–20 mb.

By comparing the calculated and measured values of the transparency ratio for the three target combinations, it is possible to determine the weighted average of the  $\phi$  width  $\Gamma_\phi$  in the nuclear rest frame for density  $\rho_0$  for each momentum bin. The results of applying this procedure are shown in Fig. 4(a) for both models 1 and 2. Model 3, as well as the SPring-8 [15] and JLab [16] data, are directly sensitive to the values of the  $\phi N$  absorption cross section that are noted in Fig. 4(b). The values of  $\Gamma_\phi$  shown in Fig. 4(a) were, in these cases, deduced in the low-density approximation,  $\Gamma_\phi = p_\phi \rho_0 \sigma_{\phi N} / E_\phi$ .

Figure 5 shows the measured differential cross sections for  $\phi$  production as functions of  $p_\phi$ . The result on the light C nucleus increases much faster with the  $\phi$  momentum than for heavier targets, and this is reflected in the variation of the transparency ratio in Fig. 2. The experimental results are compared with the predictions of the models 2 and 3 that use the values of the  $\phi$  width and  $\phi N$  absorption cross section shown in Fig. 4. The agreement of both models with the data generally improves for larger  $p_\phi$ , though, in the highest momentum bin, the results of model 3 lie closer to experiment. One possible reason for this is the introduction of a greater number of  $\phi$  production channels in this model. On the other hand, both models underestimate strongly the experimental data at low  $p_\phi$ .

The models are, of course, sensitive to the relative strength of  $\phi$  production in  $pp$  and  $pn$  collisions [25]. This is experimentally uncertain and a theoretical estimate of the

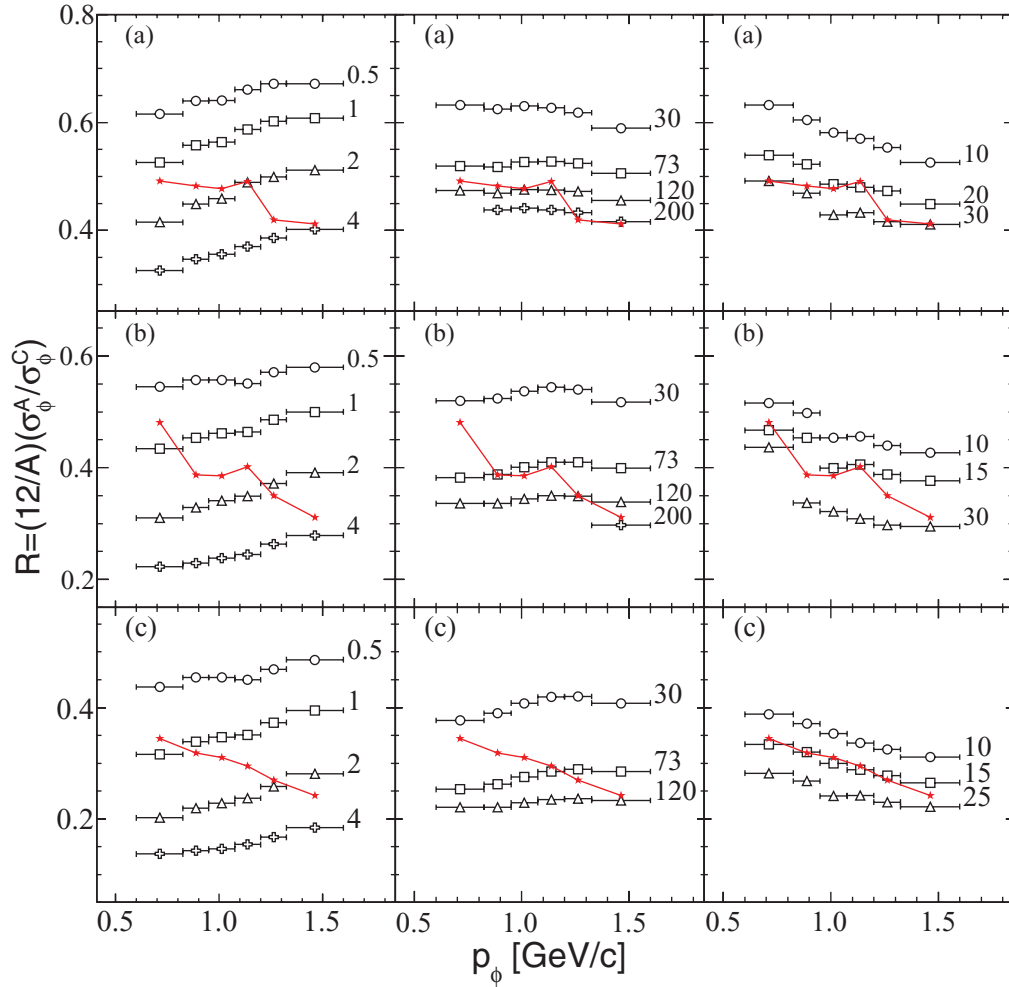


FIG. 3. (Color online) The transparency ratio  $R$  for the nuclear combinations (a) Cu/C, (b) Ag/C, and (c) Au/C as functions of the  $\phi$  laboratory momentum. The experimental data, shown in red, are connected with lines to guide the eye. The predictions of the three theoretical approaches are shown for model 1 (left), model 2 (center), model 3 (right). For the rest of the notations, see the text.

ratio [34] was used within the models. This corresponds to the cross section for  $\phi$  production in  $pn$  collisions being about four times larger than in  $pp$  collisions at 2.83 GeV. This point is particularly significant for the high-momentum components.

An alternative way to estimate the in-medium  $\phi$  width or  $\sigma_{\phi N}$  would be through a direct fit of the absolute cross sections within the framework of either model 2 or 3. It is clear that the uncertainties in the resulting parameters would be larger than those that use the transparency ratio because there are then no cancellations, either theoretical or experimental. However, calculations within these models show that, for  $p_\phi > 1$  GeV/c, the production cross sections can be described with a  $\phi$  width of about 40 MeV/c<sup>2</sup> at density  $\rho_0$ , i.e., with a  $\phi N$  absorption cross section of 15–20 mb. These values are consistent with those shown in Fig. 4. At lower momenta, the calculations in both models underestimate the data even if one takes the free value of the  $\phi$  width or a vanishing value for the  $\phi N$  absorption cross section.

The above inconsistencies suggest that some processes, whose contributions to the  $\phi$  production cross sections increase

for lower  $\phi$  momenta and with the size of the nucleus, are not present in the models. The inclusion of additional secondary production reactions, involving for example  $\omega N \rightarrow \phi N$  [18], as well as processes where the  $\phi$  slows down during its propagation through the nucleus through elastic and inelastic collisions [35], would enhance the low-momentum part of the  $\phi$  spectrum. Unfortunately, the cross sections for such processes are not known experimentally and so cannot be introduced reliably.

It can be argued that the transparency ratio is less sensitive to nuclear effects and secondary production processes than the production cross section. This may provide some justification for using the models to extract the  $\phi$  width from the experimental transparency ratio over the full momentum range studied. In fact, model 1 allows one to deduce values of  $\Gamma_\phi$  from the  $A$  dependence of  $R$ , while not making any predictions for the  $\phi$  production cross sections.

As can be seen from Fig. 4, the application of the three models yields broadly consistent results. The differences come mainly from the divergent descriptions of the secondary  $\phi$  production processes. Our findings are not inconsistent with

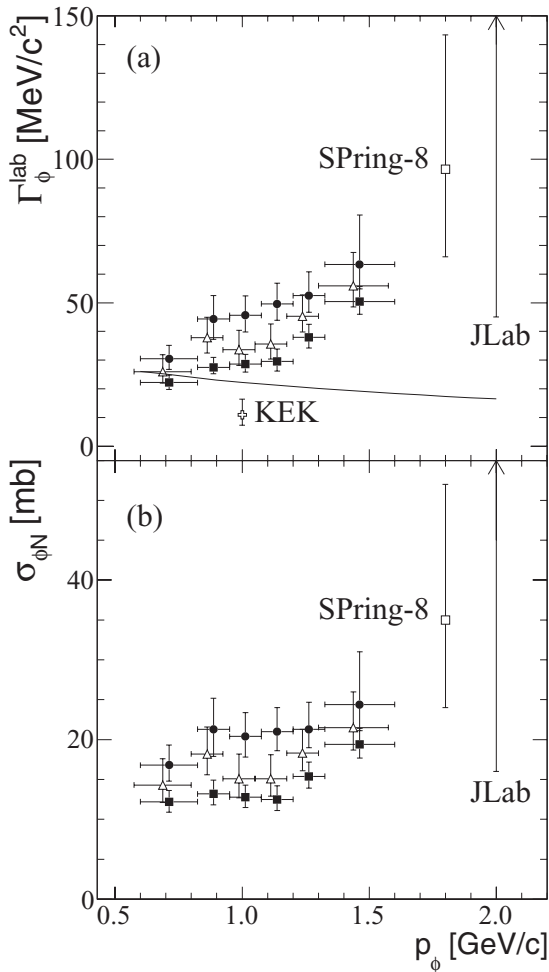


FIG. 4. (a) In-medium width of the  $\phi$  meson in the nuclear rest frame at saturation density  $\rho_0$  as a function of the  $\phi$  momentum. The points have been evaluated by comparing the data of Fig. 2 with the results of the three model calculations shown in Fig. 3 (model 1—solid squares, model 2—solid circles and model 3—open triangles). Also shown are the results from the other experiments noted [13,15,16]. The solid line represents the  $\Gamma_\phi$  calculated on the basis of the predicted  $\phi$  self-energy in nuclear matter [12]. (b) The  $\phi N$  absorption cross section. In the case of model 3, this is the parameter that is directly determined from the comparison with experiment, whereas for models 1 and 2 it is deduced from the in-medium  $\phi$  widths within the low-density approximation. The SPring-8 [15] and JLab [16] values of the cross section are also shown.

the KEK result, taking into account the uncertainties in both the experiment and in the model-dependent analysis. The observed growth of  $\Gamma_\phi$  with  $p_\phi$  is supported by the SPring-8 and JLab data. Note that the values of  $\Gamma_\phi$  extracted within the three models agree quite well with those predicted by the Valencia group [12] at  $\phi$  momenta between 0.6 and 0.825 GeV/c but deviate strongly from them at higher  $p_\phi$ , reaching a magnitude of about 50–70 MeV/c<sup>2</sup> at  $p_\phi \approx 1.5$ –1.6 GeV/c. It is worth noting that, taken together, the latest results by the CBELSA/TAPS [36] and CLAS/JLab [16] Collaborations suggest an increase also of the in-medium  $\omega$ -meson width with  $p_\omega$ .

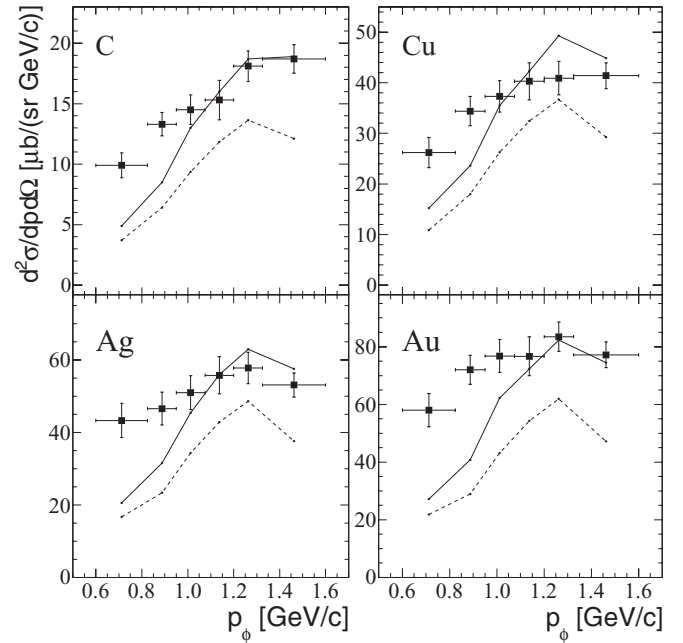


FIG. 5. Inclusive double-differential cross sections for  $\phi$  production at small angles,  $\theta_\phi < 8^\circ$ , in the collisions of 2.83 GeV protons with C, Cu, Ag, and Au targets as functions of the  $\phi$  laboratory momentum (solid squares). The errors shown are those from Table II added in quadrature. The experimental data are compared with the predictions of model 2 (dashed lines) and model 3 (solid lines) using, respectively, the central values of the  $\phi$  width and effective  $\phi N$  absorption cross section shown in Fig. 4.

Our data shows evidence for a momentum dependence of  $\sigma_{\phi N}$  and, as a consequence, our findings are not inconsistent with the results from SPring-8 and JLab. The absorption cross section is between 14 and 21 mb in the  $p_\phi$  range of 0.6–1.6 GeV/c. This is also in line with the value  $\sigma_{\phi N} > 20$  mb deduced by the CLAS Collaboration from a combined analysis of coherent and incoherent  $\phi$  production from deuterium [22].

#### IV. CONCLUSIONS

The differential cross sections for the forward production of  $\phi$  mesons by 2.83 GeV protons incident on nuclear targets have been measured at the ANKE-COSY facility. The dependence of the transparency ratio on the  $\phi$  momentum was determined over the range 0.6–1.6 GeV/c. Values of the  $\phi$  width in nuclear matter were extracted by comparing these data with calculations carried out within the available models. Independent of the model used for the analysis, the results show evidence for an increase of the  $\phi$ -meson width with its momentum. This was completely unexpected and represents possibly a significant result.

Sizable excesses have been observed in the numbers of  $\phi$  mesons produced with momenta below 1 GeV/c. These are not reproduced by the models employed and might suggest some enhancement in the low-mass  $\phi N$  systems. In order to get a deeper insight into the momentum dependence of the  $\phi$ -meson in-medium width, a better understanding of both the

$\phi$  production mechanism and its propagation through nuclear matter is crucial.

In general,  $\phi$ -meson production on hydrogen with elementary probes is not completely understood at the energy of our experiment [37,38], and this should certainly be improved. It might be interesting to note in this context that strangeness production in closely related channels might have some influence here [39–41].

## ACKNOWLEDGMENTS

This article was based in part on a Ph.D. thesis submitted by one of the authors (A.P.) to ITEP, Moscow. Support from the members of the ANKE Collaboration, as well as the COSY machine crew, are gratefully acknowledged. We are particularly appreciative of the help and encouragement that we received from Eulogio Oset. This work has been partially financed by the BMBF, COSY FFE, DFG, and RFBR.

- 
- [1] R. Rapp and J. Wambach, *Adv. Nucl. Phys.* **25**, 1 (2000).  
 [2] R. S. Hayano and T. Hatsuda, *Rev. Mod. Phys.* **82**, 2949 (2010).  
 [3] S. Leupold, V. Metag, and U. Mosel, *Int. J. Mod. Phys. E* **19**, 147 (2010).  
 [4] G. E. Brown and M. Rho, *Phys. Rev. Lett.* **66**, 2720 (1991).  
 [5] T. Hatsuda and S. H. Lee, *Phys. Rev. C* **46**, R34 (1992).  
 [6] S. Okubo, *Phys. Lett.* **5**, 165 (1963); G. Zweig, CERN Report No. TH-401, 1964 (unpublished); J. Iizuka, *Prog. Theor. Phys. Suppl.* **37**, 21 (1966).  
 [7] T. Mibe *et al.*, *Phys. Rev. C* **76**, 052202(R) (2007).  
 [8] H. Gao, T. S. H. Lee, and V. Marinov, *Phys. Rev. C* **63**, 022201(R) (2001).  
 [9] E. Oset and A. Ramos, *Nucl. Phys. A* **679**, 616 (2001).  
 [10] F. Klingl, T. Waas, and W. Weise, *Phys. Lett. B* **431**, 254 (1998).  
 [11] D. Cabrera and M. J. Vicente Vacas, *Phys. Rev. C* **67**, 045203 (2003).  
 [12] D. Cabrera, L. Roca, E. Oset, H. Toki, and M. J. Vicente Vacas, *Nucl. Phys. A* **733**, 130 (2004).  
 [13] R. Muto *et al.*, *Phys. Rev. Lett.* **98**, 042501 (2007).  
 [14] E. Ya. Paryev, *Eur. Phys. J. A* **23**, 453 (2005).  
 [15] T. Ishikawa *et al.*, *Phys. Lett. B* **608**, 215 (2005).  
 [16] M. H. Wood *et al.*, *Phys. Rev. Lett.* **105**, 112301 (2010).  
 [17] C. B. Dover, J. Hüfner, and R. H. Lemmer, *Ann. Phys. (NY)* **66**, 248 (1971).  
 [18] A. Sibirtsev, H. W. Hammer, U.-G. Meißner, and A. W. Thomas, *Eur. Phys. J. A* **29**, 209 (2006).  
 [19] P. Mühlich and U. Mosel, *Nucl. Phys. A* **765**, 188 (2006).  
 [20] H.-J. Behrend *et al.*, *Nucl. Phys. B* **144**, 22 (1978).  
 [21] H. J. Lipkin, *Phys. Rev. Lett.* **16**, 1015 (1966).  
 [22] X. Qian *et al.*, *Phys. Lett. B* **680**, 417 (2009).  
 [23] W. C. Chang *et al.*, *Phys. Lett. B* **684**, 6 (2010).  
 [24] X. Qian *et al.*, *Phys. Lett. B* **696**, 338 (2011).  
 [25] A. Polyanskiy *et al.*, *Phys. Lett. B* **695**, 74 (2011).  
 [26] V. K. Magas, L. Roca, and E. Oset, *Phys. Rev. C* **71**, 065202 (2005).  
 [27] E. Ya. Paryev, *J. Phys. G* **36**, 015103 (2009).  
 [28] H. Schade, Ph.D. thesis, University of Dresden, 2010 (unpublished) [[http://slubdd.de/katalog?libero\\_mab215140804](http://slubdd.de/katalog?libero_mab215140804)].  
 [29] M. Hartmann *et al.*, *AIP Conf. Proc.* **1322**, 349 (2010).  
 [30] S. Barsov *et al.*, *Nucl. Instrum. Methods Phys. Res., Sect. A* **462**, 364 (2001).  
 [31] M. Hartmann *et al.*, *Int. J. Mod. Phys. A* **22**, 317 (2007).  
 [32] M. Büscher *et al.*, *Nucl. Instrum. Methods Phys. Res., Sect. A* **481**, 378 (2002).  
 [33] A. Polyanskiy *et al.*, in *Proceedings of the XIV International Conference on Hadron Spectroscopy, Munich*, 2011, edited by B. Grube, S. Paul, and N. Brambilla, eConf C110613 (2011) [<http://www.slac.stanford.edu/econf/C110613/>].  
 [34] L. P. Kaptari and B. Kämpfer, *Eur. Phys. J. A* **23**, 291 (2005).  
 [35] P. Mühlich, T. Falter, C. Greiner, J. Lehr, M. Post, and U. Mosel, *Phys. Rev. C* **67**, 024605 (2003).  
 [36] M. Kotulla *et al.*, *Phys. Rev. Lett.* **100**, 192302 (2008).  
 [37] T. Mibe *et al.*, *Phys. Rev. Lett.* **95**, 182001 (2005).  
 [38] B. Dey and C. A. Meyer, *AIP Conf. Proc.* **1388**, 242 (2011).  
 [39] B. Dey *et al.*, *Phys. Rev. C* **82**, 025202 (2010).  
 [40] S. A. Pereira *et al.*, *Phys. Lett. B* **688**, 289 (2010).  
 [41] H. Kohri *et al.*, *Phys. Rev. Lett.* **104**, 172001 (2010).